Spherically symmetric wormholes with anisotropic matter

Hyeong-Chan Kim and Youngone Lee[1]

School of Liberal Arts and Sciences, Korea National University of Transportation, Chungju 380-702, Korea

E-mail: hyeongchan@gmail.com, youngone@ut.ac.kr

Abstract. We study the geometry of a wormhole spacetime filled with anisotropic matter in the context of general relativity. In the course of the study, new static and spherically-symmetric solutions, analytic and numerical ones, are found. We specify the existence condition for a wormhole throat. We analyze properties of the solutions after categorizing them based on the spacetime regularity and the signature of energy density. The necessary conditions which allow a wormhole spacetime to be nonsingular are described.

---

[1]Corresponding author.

Contents

1 Introduction

Wormhole spacetimes are solutions of general relativity [1–6] which differ from other solutions such as massive stars and black holes. The key difference lies in the topology. Two asymptotic regions are connected by a passage called a 'throat'. Since general relativity is a local theory, it does not tell what the topology of whole spacetime should be and does not exclude wormhole spacetimes.

Although wormholes are genuine solutions of general relativity, the study of wormholes had not drawn much interest of researchers until recently. The main reason is that the existence of wormhole requires violation of energy conditions, which are strong constraints to matter based on human intuitions on ordinary classical matter. To pass a throat of a wormhole, the geodesics of light bundle converge and then diverge which requires 'exotic' or 'phantom' matter having negative pressure [2, 7]. Another reason is that this unique topology obscures many previously accepted physical concepts. One may construct a time machine [2, 8], may have 'charge without charge' [9] and the ADM mass measured in one side of the wormhole may not be identical to that in the other side [8, 10].

Despite of this pathology, researchers in this field have studied wormholes as physical objects in the hope of future resolution of energy conditions. Recently, an attempt to construct 'phantom free models' was suggested [11] while others have tried to get around the

pathology by constructing a wormhole using 'ordinary' matter in modified theories of gravity [12–16]. On the other hand, in quantum world, many examples were found which allow the violation of energy conditions. Casimir effect [17], negative energy region of squeezed light [18] and the dark energy are the most prominent examples. Therefore, the violation of the energy condition is acceptable for such special circumstances.

Recently, wormholes have drawn interests as a test-bed to understand quantum entanglement. A non-traversable wormhole is regarded as a pair of entangled black holes in 'ER=EPR' conjecture to understand the information paradox [19]. Traversable wormholes have also been suggested to have physically sensible interpretation of the conjecture [20]. The study of wormholes as physical entities in understanding the quantum-gravity is getting more important than ever at this juncture.

Our purpose in this paper is, as a preliminary step, to categorize wormhole solutions and study the characteristic features of those solutions to attain more clear grasp of the physical aspects of wormholes. We focus on static, spherically symmetric traversable wormholes which consist of anisotropic matter in the context of general relativity. The anisotropic matter we are considering here satisfies linear equation of state throughout the entire space. Hence isotropic perfect fluid is a special case of our study. Although the anisotropic matter is distributed throughout the entire space, one can obtain a spacetime of desirable asymptotic properties or of minimal 'exotic' matter with appropriate junction conditions to match a truncated solution of us [21].

Traditionally wormhole solutions have been obtained after assuming a well-behaving wormhole metric first then calculating the Riemann tensor to get an appropriate stress-energy tensor for matter fields afterward [22]. On the other hand, in this work, we begin with the specification of matter fields satisfying a given equation of state and then solve Einstein's equation. After that, we find out the condition for a wormhole solution to be nonsingular over the whole spacetime. We also analyze properties satisfied by the general solutions and categorize them into six types based on the spacetime regularity and the signature of energy density.

The existence condition for a wormhole throat and properties of Einstein equation are discussed in section 2. Analysis of general solutions is in section 3 where behavior of solutions around special points such as points at asymptotes, the throat and the repelling point are analyzed. Numerical solutions are also presented in section 4 and a few exact solutions are presented in section 5. Properties of a few limiting solutions are presented in section 6. Finally, we summarize the results and discuss the properties of the solutions and suggest future works to be done in section 7.

2 General properties and existence conditions

For simplicity, we consider static and spherically symmetric configurations. The stress-energy tensor for an anisotropic fluid compatible with the spherical symmetry is given by

$$T^{\mu\nu} = \rho u^\mu u^\nu + p_1 r^\mu r^\nu + p_2(\theta^\mu \theta^\nu + \phi^\mu \phi^\nu), \tag{2.1}$$

where ρ is the energy density measured by a comoving observer with the fluid. The vectors u^μ, r^μ, θ^μ and ϕ^μ are mutually orthogonal and denote four-velocity, radial and the unit angular vectors, respectively. As we mentioned above, the radial and the angular pressures are assumed to be proportional to the density:

$$p_1 = w_1 \rho, \qquad p_2 = w_2 \rho, \tag{2.2}$$

with constant w_1 and w_2. We focus on a static and spherically symmetric configuration of which the line element[1] is given by

$$ds^2 = -f(r)dt^2 + \frac{1}{1 - 2m(r)/r}dr^2 + r^2 d\theta^2 + r^2 \sin^2 \theta d\phi^2. \tag{2.3}$$

2.1 Tolmann-Oppenheimer-Volkhoff equation

The G_{tt} part of the Einstein equation defines the mass function $m(r)$ as,

$$m(r) = 4\pi \int^r r'^2 \rho(r')dr', \tag{2.4}$$

where an integration constant is absorbed into the definition of $m(r)$. The continuity equation $\nabla^\mu T_{\mu\nu} = 0$ yields the Tolmann-Oppenheimer-Volkhoff (TOV) equation for an anisotropic matter,

$$p_1' = -(\rho + p_1)\frac{m + 4\pi r^3 p_1}{r(r - 2m)} + \frac{2(p_2 - p_1)}{r}. \tag{2.5}$$

Here the prime means to take the derivative with respect to r.

Then g_{tt} part of the metric, or $f(r)$, can be obtained in two different ways. Combining the relation $G_{tt} = 8\pi T_{tt}$ and $G_{rr} = 8\pi T_{rr}$ we have

$$\frac{f'}{f} = \frac{2(m + 4\pi r^3 p_1)}{r(r - 2m)}. \tag{2.6}$$

The equation can be directly integrated to give

$$f(r) = \tilde{f}_0 \frac{(r - 2m)^{-w_1}}{r} \exp\left[(1 + w_1)\int_{r_0}^r \frac{1}{r - 2m(r)}dr\right], \tag{2.7}$$

where $\tilde{f}_0$ is an integration constant. The w_2-dependence will be restored in (2.7) when $m(r)$ is expressed explicitly. The sign of $\tilde{f}_0$ will be chosen so that the signature of the metric be Lorentzian because the Einstein equation does not determine the sign of $f(r)$. On the other hand, the anisotropic TOV equation (2.5) with the equation of state (2.2) reads

$$\frac{\rho'}{\rho} = -\frac{1 + w_1}{2w_1}\frac{f'}{f} + \frac{2(w_2 - w_1)}{w_1}\frac{1}{r}.$$

After integrating one gets

$$f(r) = f_b \left(\frac{r}{b}\right)^{\frac{4(w_2 - w_1)}{1 + w_1}} \left(\frac{\rho}{\rho_b}\right)^{-\frac{2w_1}{1 + w_1}}, \tag{2.8}$$

where b is the value of the radial coordinate at the throat. Here, ρ_b and f_b are the values of energy density and the function f at the throat. We have two forms of $f(r)$, (2.7) and (2.8), and both are useful for later considerations.

The remaining task is to find the explicit form of $m(r)$ by solving the TOV equation.[2] Using eqs. (2.2) and (2.4), the TOV equation becomes

$$\frac{m''}{m'} = -\frac{1 + w_1}{2w_1}\frac{1 + 2w_1 m'}{r - 2m} + \frac{1 + w_1 + 4w_2}{2w_1 r}, \tag{2.9}$$

---

[1]Because we deal with spherically symmetric situation, many parts of the calculation in this section overlap with those in ref. [23]. Therefore, we leave only the main results.

[2]When $w_1 = -1$ and $w_1 = -1/3 = w_2$, the TOV equation allows exact solutions as in refs. [24, 25].

where we use $\rho'/\rho = m''/m' - 2/r$. Equation (2.9) does not allow an analytic solution in general. However, the above relation can be cast into a first order autonomous equation in a two dimensional (u, v) plane:

$$\frac{du}{dv} = \frac{-1}{1 + w_1} \frac{(1 - u)(2v - u)}{v\left[v - v_b + s(1 - u)\right]}, \tag{2.10}$$

where u and v are scale-invariant variables defined by

$$u \equiv \frac{2m(r)}{r}, \qquad v \equiv \frac{dm(r)}{dr} = 4\pi r^2 \rho. \tag{2.11}$$

The constants v_b and s denote the value of v at the wormhole throat and the *slope* of the line $v - v_b + s(1 - u) = 0$, respectively,

$$v_b \equiv -\frac{1}{2w_1}, \qquad s \equiv -\frac{1 + w_1 + 4w_2}{2w_1(1 + w_1)}. \tag{2.12}$$

Given u and v, the metric g_{tt} can be reconstructed from v via eq. (2.8) and g_{rr} from u respectively.

2.2   The existence condition for a wormhole throat

The geometry of each side of the throat is described by the metric (2.3) with an appropriate mass function. For the metric (2.3) to have a throat at $r = b$, its spatial part should have a coordinate singularity of the form $g_{rr} \approx g(1 - b/r)^{-1}$ with $g > 0$ where r is an areal radial coordinate.[3] We then, from eq. (2.7), find

$$f(r) \propto \frac{g^{w_1}}{r}(r - b)^{(1+w_1)g - w_1}.$$

At the wormhole throat, $f(b)$ should take a finite value, hence the value of g becomes

$$g \equiv \lim_{r \to b} \left(1 - \frac{b}{r}\right) g_{rr} = \frac{w_1}{1 + w_1} > 0.$$

Therefore, a wormhole solution exists only when $w_1 < -1$ or $w_1 > 0$.[4] Around the throat, the mass function $m(r)$ behaves as, from $g_{rr} = (1 - 2m(r)/r)^{-1}$,

$$m(r) \simeq \frac{b}{2w_1}\left(1 + w_1 - \frac{r}{b}\right) \quad \Rightarrow \quad m'(b) = -\frac{1}{2w_1}. \tag{2.13}$$

From this, one can notice that the value of $v \equiv m'(r)$ at the wormhole throat is solely determined by w_1.[5] Previous definition of $v_b(= -1/2w_1)$ comes from this observation.

---

[3]Consider $g_{rr} \approx g(1 - b/r)^{-\beta}$. When $\beta < 1$ and $\beta \neq 0$, the geometry must be singular [23]. When $\beta \geq 2$, the geometry at $r = b$ can be regular but the surface $r = b$ is located at infinity implying that the throat is non-traversable. Therefore, to be traversable, the value should satisfy $1 \leq \beta < 2$. However, when β is non-integer, higher curvatures must have a singularity at $r = b$. In this sense, we restrict our interest to $\beta = 1$ case to find a nonsingular traversable wormhole.

[4]When $w_1 = 0$ and $g = 0$, the spatial geometry does not form a throat at b. The solution for $w_1 = -1$ was analyzed in ref. [25] thoroughly in which no wormhole-like solutions were found.

[5]One can confirm that all three solutions in ref. [1] satisfy this relation. For the case that w_1 depends on r, $w_1 = w_1(r)$ as in ref. [27], one can show that $m'(b) = -1/2w_1(b)$.

Based on the observation above, let us divide the wormhole 'throats' into two types:

1. When $w_1 > 0$ ($v_b < 0$): the mass function decreases from $b/2$ with r, meaning that the mass in the region $(b, R > b)$ is $\Delta m = m(R) - m(b) < 0$. The energy density at the throat takes a negative value $\rho(b) = v_b/4\pi b^2 < 0$.

2. When $w_1 < -1$ ($0 < v_b < 1/2$): the mass function increases with r and the density takes a positive value. Therefore, if we use matter with positive energy density to weave a wormhole throat, we cannot avoid phantom-like matter satisfying $w_1 < -1$.

As we have commented previously, we consider nonsingular solutions in which all quantities are continuous throughout the entire spacetime. If necessary, solutions with a surface layer or discontinuous energy of a hypersurface [21] can be obtained by cut and paste our solutions with appropriate junction conditions. To express both sides of the throat continuously, one may introduce a new radial coordinate x around the throat,

$$\sqrt{g_{rr}(r)}dr = \pm b dx \quad \Rightarrow \quad \pm x \simeq 2\sqrt{g}\sqrt{\frac{r}{b} - 1}, \tag{2.14}$$

where we choose $x = 0$ at the throat and $\pm$ for $x \gtrless 0$, respectively. This gives

$$\frac{dm(x)}{dx} = \frac{dr(x)}{dx} m'(r) = \frac{-(1 + w_1)}{4w_1^2} x.$$

Therefore, there is no singularity or discontinuity of density at the wormhole throat. Note that the existence condition for a wormhole throat is independent of the angular pressure.

It is to be noted that the radial coordinate does not have to be areal to show the inevitable use of 'exotic' matter. As in ref. [26], the violation of energy conditions can also be derived by requiring $r(x)$ to be a minimum at the throat with respect to the regular x-coordinate combining with the Einstein equations. The use of areal radial coordinate here enables us to show the independence of the angular pressure at the throat threaded by anisotropic matter. In other words, the angular pressure can have any value that makes the solution be nonsingular.

3   Analysis for general solutions

The solution to the autonomous equation (2.10) can be represented by an integral curve C on the two dimensional plane (u, v). Hence, to sketch general properties of solutions we need to closely look at the autonomous equation.

There are four interesting lines on which the denominator or the numerator is equal to zero or equivalently, $dv/du = 0$ or $du/dv = 0$. These four lines are plotted in figures 1 and 2. We call the thick-red lines R1 and R2 on which only u changes its value ($dv/du = 0$) and C crosses the lines horizontally:

$$\text{R1: } v = 0, \qquad \text{R2: } v - v_b = s(u - 1). \tag{3.1}$$

Energy density $\rho \propto v$ vanishes on the line R1. Because R1 is horizontal, solution curves are allowed to touch R1 only at a special points $\mathcal{O}(0, 0)$ and $P_E(1, 0)$ because $dv/du = 0$ on R1.

We call the thick-black lines B1 and B2 on which only v changes its value ($du/dv = 0$) and C crosses the lines vertically:

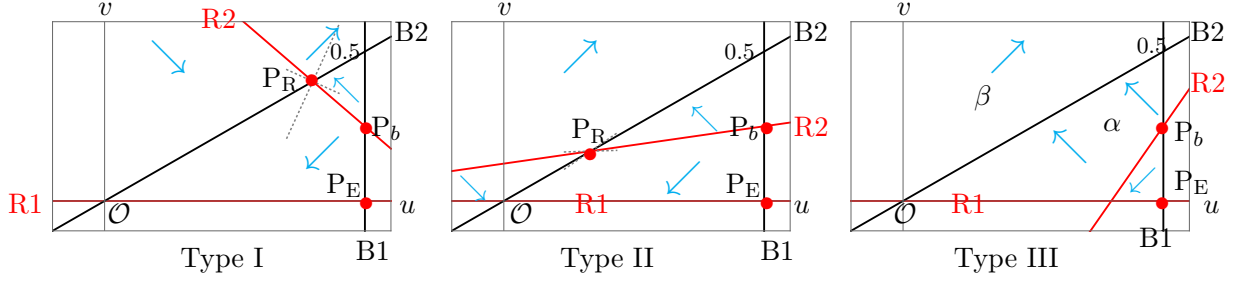$$\text{B1: } u = 1, \qquad \text{B2: } u = 2v. \tag{3.2}$$

Figure 1. Classification of the autonomous equation for $w_1 < -1$. The cyan arrows represent the increasing direction of radial coordinate r. The direction changes based on the lines B2 and R2. The red line R2 changes depending on the values of w_i.

The line B1 represents a static boundary where g_{rr} changes its signature. Because the line B1 is parallel to the v axis, C is allowed to cross the line only through P_E, where the subscript E denotes event horizon. Since we focus on static traversable wormhole solutions in this work, we restrict our interests to the region with $u \leq 1$. As will be shown later in this work, a solution having a traversable wormhole throat does not have an event horizon, i.e., its solution curve never crosses B1.[6] Note that solution curves never become vertical or horizontal at the points which are not on the lines R1, R2, B1, and B2.

The crossing points between the black lines and the red lines are

$$\mathcal{O}(0,0), \quad P_E(1,0), \quad P_b\big(1, v_b\big), \quad P_R(2v_R, v_R), \tag{3.3}$$

where $v_R \equiv 2w_2/[(1 + w_1)^2 + 4w_2]$. The point $\mathcal{O}$ plays the role of an asymptotic geometry of $r \to \infty$ for the wormhole spacetime. The point P_b is a wormhole throat. The point P_R is a point where B2 meets R2 and acts like a 'repeller' as described in section 3.3.3. Because solutions tend to avoid this point, we call P_R 'Repelling point'. The radial dependence of a solution curve C on the (u, v) plane can be obtained from

$$\frac{dr}{r} = \frac{du}{2v - u} = \frac{-1}{1 + w_1} \frac{1 - u}{v[v - v_b + s(1 - u)]} dv, \tag{3.4}$$

where the second equality comes from eq. (2.10). The relation can be interpreted as:

- The radius increases/decreases with u when the curve is above/below the line B2, respectively.

- The radius increases or decreases with v depending on many factors. They are the signature of $1 + w_1$ and whether the curve is above or below the lines R1 and R2.

Hence, the region $(u < 1, v)$ is divided into 7 regions maximally by the 3 lines, R1, R2 and B2. The increasing direction of r varies region by region. The 'cyan' arrows in the figures in this work represent the increasing direction of r. One can intuitively notice how the solution (mass and density) develops as one moves from the throat to the outside regions.

---

[6]If the equation of state is nonlinear, or w_1, w_2 are functions of r as in ref. [6], a wormhole spacetime having a cosmological horizon could exist. At the present work, any solution curve having a wormhole throat, does not go into the time dependent region. In other words, the sign of temporal component of the metric, g_{tt}, does not change here(For details see footnote 7). To be specific, we consider the theory of general relativity without cosmological constant and matter with constant equation of states w_1 and w_2 satisfying $w_1 < -1$ or $w_1 > 0$.

As an example, let us apply the above properties to the Type I and II of the figure 1. Consider a solution curve which passes P_b vertically. If it goes vertically upwards from P_b, the solution curve C bends to the left following the cyan arrow until the curve meets the line B2 or R2. If it touches the line B2, the curve bends upwards and approaches the line B1 indefinitely. This asymptotic behavior with $v = m'(r) \to \infty$ can be excluded as a physically viable regular solution. By applying the same consideration, one can figure out genuine regular solutions.

3.1 Analysis for $w_1 < -1$ and $\rho > 0$

Let us first consider the case with $w_1 < -1$. In this case, $v_b > 0$. In terms of the slope s of the line R2, we divide the deployment of the points and the lines into three different types as in figure 1,

$$\text{I: } s < 0 \ \left(w_2 > -\frac{1 + w_1}{4} \right), \quad \text{II: } 0 \leq s \leq v_b \ \left(0 \leq w_2 \leq -\frac{1 + w_1}{4} \right), \quad \text{III: } s > v_b \ (w_2 < 0).$$

For the Types I and II the point P_R is in the region we are interested in($0 \leq u < 1$). For the Type III, P_R is located outside of the region. In section 5, we present and display exact solutions which belong to the types I and II.

Even though there is a wormhole throat, the solutions in the Type III does not have a regular asymptotic region: most of the solution curves allowing a wormhole throat pass the point P_b with $u \leq 1$ and tangent to the line B1 at the throat except a symmetric solution described in section 3.3.2. Let us consider one of the curves. A solution curve may depart from P_b vertically upwards (increasing v, decreasing u) and downwards (decreasing u and v). As one can see clearly from the arrows, the first one that starts from the region α continues until it meets the line B2 and becomes vertical followed by entering the region β. Once a solution curve enters the region β it goes upwards to a singular region $v \to \infty$ until the curve becomes parallel to the line B1 ($u = 1$). The second one touches R2 at some point,[7] and becomes horizontal there entering to the region α. In this region, v cannot decrease but only increases until C meets the line B2. There, C becomes vertical again and enters the region β and repeats the same behavior as above. In summary, both ends of C give infinity value of v, implying singularities. Therefore, later in this work, we consider only the type I and II with $w_2 \geq 0$.

3.2 Analysis for $w_1 > 0$ and $\rho < 0$

In this case, since $v_b < 0$, the energy density near the wormhole throat is negative. There are three types:

$$\text{IV: } s > 0 \ \left(w_2 < -\frac{1 + w_1}{4} \right), \quad \text{V: } v_b \leq s \leq 0 \ \left(-\frac{1 + w_1}{4} \leq w_2 \leq 0 \right), \quad \text{VI: } s < v_b \ (w_2 \geq 0).$$

We first show that the Type VI does not allow a regular wormhole solution as in the Type III for $w_1 < -1$. Let us consider a solution curve C passing P_b vertically. Vertically upward part of the curve becomes horizontal when it meets the red lines R1 or R2. As can

---

[7]If the curve C touches R1, it is possible only at P_E in principle. This is not possible because the autonomous equation implies that the solution is analytic. Putting the trial function $u = 1 - \kappa|v|^\beta$ with $\kappa|v|^\beta \ll 1$ to eq. (2.10) we get $\beta = (-2w_1)/(1 + w_1) < 0$. Therefore, the solution curve C never meet the point P_E but bounces for any value of $\kappa \neq 0$. This implies that event horizons will never be formed.
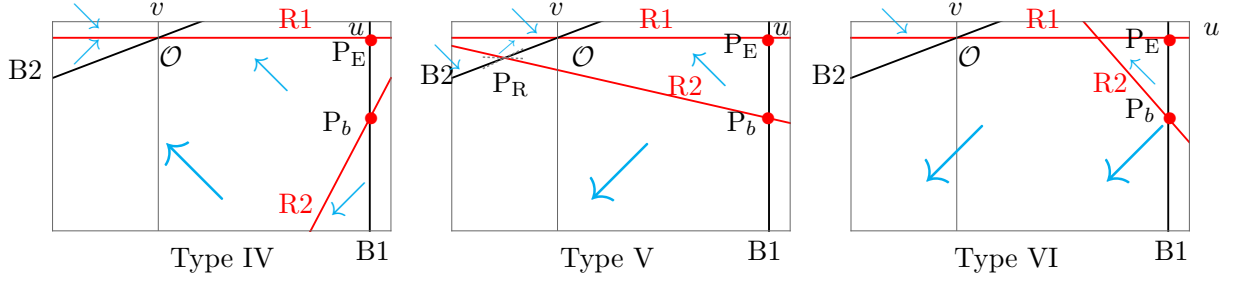
Figure 2. Classification of the autonomous equation for $w_1 > 0$. The direction changes based on the line B2, R1 and R2.

be understood in the figure, the curve will cross R2 before it meets $\mathcal{O}$ and becomes parallel to the u axis. Then, by similar consideration above (when $w_1 < -1$), the solution curve after crossing the line R2 goes to the region $(u,v) \to (-\infty, -\infty)$. Vertically downward part of the curve at P_b cannot be a parallel to the $v = 0$ line because it never meet a red line. Again, the curve goes to the region $(u,v) \to (-\infty, -\infty)$. In this case, a space-time singularity will form there.

On the other hand, for the type IV, the vertically upward part of C can approach $\mathcal{O}$, hence some solutions follow the path. The vertically downward part of C can meet R2 and becomes parallel and the value v starts to increase. In that case, some curve can also approach the point $\mathcal{O}$. Therefore, there are possibilities that both ends of a solution curve finish at $\mathcal{O}$, forming regular asymptotic regions. Similar analysis for the type V leads that only upward curves have a possibility to approach $\mathcal{O}$, to form a regular solution.

To summarize, we are mainly interested in the cases with Type I, II, IV, and V. For all the cases, $w_1 w_2 < 0$ is satisfied. Therefore, isotropic fluid fails to form a regular wormhole spacetime.

3.3 Behaviors around important points

To have clear pictures, we study properties of solutions around a few important points. One of them is $\mathcal{O}$ which represents asymptotic limit $(r \to \infty)$ for the types I, II, IV and V. Other important points are P_b and P_R, representing a wormhole throat and the repelling point, respectively.

3.3.1 The asymptotic behavior around $\mathcal{O}$

Let us first search for the behavior of C around the point $\mathcal{O}(0,0)$. Because $|u|, |v| \ll 1$ around $\mathcal{O}$, eq. (2.10) can be approximated as

$$u'(v) = \alpha \left(\frac{u}{v} - 2 \right), \quad \alpha = -\frac{w_1}{2w_2}. \tag{3.5}$$

Solving the equation gives

$$u = \begin{cases} \dfrac{2\alpha}{\alpha - 1} v + q \left(\dfrac{v}{v_b} \right)^{\alpha} & (\alpha \neq 1), \\[3mm] -2v \log |v| + q' \, v & (\alpha = 1), \end{cases} \tag{3.6}$$

– 8 –

where q and q' are integration constants. Because we are interested only in $w_1 w_2 < 0$ case, the constant α takes positive value ($\alpha > 0$).[8] The solution curve of a regular wormhole should not end in the region $u \to -\infty$ or $v \to \infty$. Thus, both ends of a solution curve should be located at $\mathcal{O}$. In this sense, the point $\mathcal{O}$ plays the role of an asymptotic infinity.

In eq. (3.6), when $\alpha > 1$, the linear behavior dominates since $v^\alpha \ll 1$. When $0 < \alpha < 1$, the power law behavior (the v^α term) dominates. When $\alpha = 1$, the solution takes $u \sim -2v \log |v|$ behavior.

The radius can be expressed in terms of v as

$$r = r_0 \left(\frac{v}{v_b} \right)^{-\alpha},$$

where r_0 is a constant. The mass function at r becomes

$$m(r) = \frac{ur}{2} = \frac{r_0}{2} \left[q - \frac{2\alpha}{1-\alpha} \left(\frac{r}{r_0} \right)^{(\alpha-1)/\alpha} \right]. \tag{3.7}$$

When $\alpha \geq 1$ ($0 < w_2 \leq -w_1/2$), the mass function diverges and the geometry may not be flat asymptotically. This mass function approaches a finite value $qr_0/2$ asymptotically only when $0 < \alpha < 1$ ($-2w_2 < w_1 < 0$ or $0 < w_1 < -2w_2$).

To see the g_{tt} part of the metric around $\mathcal{O}$, we need to consider the next order form of $r(v)$. It can be calculated by integrating eq. (3.4) incorporating the relation eq. (3.6) with $0 < \alpha < 1$:

$$r = r_0 \left(\frac{v}{v_b} \right)^{-\alpha} \exp \left[\frac{(1+w_1)\alpha q}{2w_1} \left(\frac{v}{v_b} \right)^\alpha \right],$$

$$\left[\frac{v(r)}{v_b} \right]^\alpha = \frac{r_0}{r} - \frac{(1+w_1)\alpha q}{2w_1} \left(\frac{r_0}{r} \right)^2 + \frac{3}{2} \left(\frac{(1+w_1)\alpha q}{2w_1} \right)^2 \left(\frac{r_0}{r} \right)^3 + \cdots . \tag{3.8}$$

Then, the g_{tt} part of the metric around $\mathcal{O}$ becomes

$$f(r) = f_0 \left(\frac{r}{r_0} \right)^{\frac{4w_2}{1+w_1}} \left(\frac{v}{v_b} \right)^{-\frac{2w_1}{1+w_1}}$$

$$= f_0 \left(1 - \frac{2m_\infty}{r} \right) + \mathcal{O} \left(\frac{1}{r^2} \right), \tag{3.9}$$

where we use eq. (2.8) with the relation $v = 4\pi r^2 \rho$ and $m_\infty = r_0 q$ denotes the asymptotic value of mass in eq. (3.7). This guarantees asymptotic flatness for $0 < \alpha < 1$ case.

The density becomes

$$\rho = \frac{v}{4\pi r^2} = \frac{1}{4\pi r_0^2} \left(\frac{r_0}{r} \right)^{2-2w_2/w_1} .$$

3.3.2 Behavior around the wormhole throat P_b

Let us investigate the behavior of a solution curve C around the throat $\mathrm{P}_b(1, v_b)$. By using the trial function $1 - u = \kappa |v - v_b|^\beta$ around $u \sim 1$, we find that eq. (2.10) allows a quadratic and a linear behaviors for C,

$$\text{i) The symmetric solution} \quad \beta = 1, \quad u = 1 - s^{-1}(v - v_b), \tag{3.10}$$

$$\text{ii) The asymmetric solution} \quad \beta = 2, \quad u = 1 - \kappa(v - v_b)^2, \tag{3.11}$$

---

[8]It is to be noted that when $\alpha < 0$, eq. (3.6) implies that the solution curve never passes the point $\mathcal{O}$ unless $q = 0$. Therefore, only linear behavior exists at $\mathcal{O}$.

where κ denotes an arbitrary real number and s is given in eq. (2.12). Here 'asymmetric'/'symmetric' implies that the geometric structure is asymmetric/symmetric with respect to the inversion relative to the throat, respectively.

For the two cases, the radius takes the form,

$$r \approx b \left[1 + \frac{w_1}{1 + w_1}(1 - u) \right].$$

(3.12)

Therefore, r takes minimum value at $v = v_b$ when $\kappa > 0$ for the case ii). As will be shown in the numerical plot, the symmetric solution appears as a large κ limit of the asymmetric solution. The example of the exact symmetric solution will be given in eq. (5.4) when $1 + w_1 + 2w_2 = 0$ i.e. $s = -v_b$.

It appears that u, v and du/dv are continuous at P_b even for solution curves with different κ. Therefore one should check whether solutions with different κ can be attached smoothly to form a proper wormhole solution or not. To answer this question, let us calculate the extrinsic curvatures. As in ref. [21] we divide a wormhole spacetime into upper/lower parts with respect to the throat and denote them $\Sigma_\pm$, respectively. Then in our coordinates, the extrinsic curvatures are

$$K_{ab}^\pm = \frac{1}{2} \frac{\partial g_{ab}^\pm}{\partial r}, \qquad a = t, \theta, \phi.$$

(3.13)

Since $K_{\theta\theta}$ and $K_{\phi\phi}$ have the same values on both sides, we consider K_{tt} only here. From the metric eq. (2.3) and the form of g_{tt} in eq. (2.8), we have

$$K_{tt} = -\frac{1}{2} \frac{df}{dr} = \left(-\frac{2w_2}{1 + w_1} \frac{1}{r} + \frac{w_1}{1 + w_1} \frac{1}{v} \frac{dv}{dr} \right) f(r).$$

(3.14)

By using eq. (3.4) and the above relations (3.10), (3.11), K_{tt} behaves as

$$K_{tt} = \begin{cases} \dfrac{1 + w_1 + 2w_2}{1 + w_1} \dfrac{f(b)}{b}, & \beta = 1, \\[3mm] -\dfrac{w_1}{\kappa(v - v_b)} \dfrac{f(b)}{b}, & \beta = 2. \end{cases}$$

(3.15)

Thus for $\beta = 1$ case, two solutions can be attached smoothly. However, for $\beta = 2$ case, the boundaries require a 'surface layer' if $K_{ab}^+ \neq K_{ab}^-$. In other words, the upper/lower parts cannot be adjoined for different κ's.

3.3.3 Behavior around the repelling point P_R

The repelling point P_R is where B2 meets R2. In ref. [28], this crossing point was shown to act as an 'attractor' in the dynamics of self-gravitating ball of radiation that a solution curve approaches P_R in a spiral form. On the other hand, in wormhole spacetimes, solution curves rather avoid P_R than take the spiral behavior. In this sense, the point P_R acts as a 'repeller'.

Let us approximate the differential equations (2.10) and (3.4) around P_R. After setting $u = u_B + x$ and $v = v_B + y$, they can be written as, to the linear order in x and y,

$$\frac{d}{d \log r} \begin{pmatrix} x \\ y \end{pmatrix} = \begin{pmatrix} -1 & 2 \\ (1 - \gamma)s & \gamma - 1 \end{pmatrix} \begin{pmatrix} x \\ y \end{pmatrix}, \qquad \gamma \equiv 1 - \frac{2w_2}{1 + w_1} = \frac{3}{2} + w_1 s > 0. \quad (3.16)$$

Defining new variables $X_\pm = y - \frac{\gamma \pm \sqrt{\gamma^2 + 8s(1-\gamma)}}{2s(1-\gamma)} x$, eq. (3.16) is reduced to a diagonal form,

$$\frac{dX_\pm}{d\log r} = \epsilon_\pm X_\pm; \qquad \epsilon_\pm = \frac{-2 + \gamma \mp \sqrt{\gamma^2 + 8s(1-\gamma)}}{2}. \tag{3.17}$$

Note that the term in the square-root is

$$D \equiv \gamma^2 + 8s(1-\gamma) = w_1(w_1 - 8)(s - s_+)(s - s_-), \tag{3.18}$$

where

$$s_\pm = \frac{4 - 3w_1 \pm 4\sqrt{1 + 3w_1}}{2w_1(w_1 - 8)}. \tag{3.19}$$

If $D < 0$, the eigenvalues $\epsilon_\pm$ have imaginary parts and the solution curve C has a spiral behaviors asymptotically as depicted in ref. [28]. In our case, this never happens. The proof is the following:

- $w_1 < -1$. Interpreting D as a quadratic function of real number s, one can find that $D = 0$ does not have a real valued solution. Hence D is always positive because $w_1(w_1 - 8) > 0$. Therefore, when $w_1 < -1$, one never gets a 'spiral' solution.

- $w_1 > 0$. In this case, $s_\pm$ are real numbers.

  1. $0 < w_1 < 8$, $(s_+ < s_-)$. In order for $D > 0$, s should satisfy $s_+ < s < s_-$. As seen in figure 2, the point P_R is located in a physical region only for the type V, which restricts $v_b \leq s \leq 0$. At the present case, $s_+ < v_b$ and $s_- > 0$. Therefore, D is positive definite.

  2. $w_1 = 8$. In this case, $D = 0$ and the eigenvalues are real-valued with $\epsilon_+ = \epsilon_-$.

  3. $w_1 > 8$, $(s_- < s_+)$. In order for $D > 0$, $s < s_-$ or $s > s_+$. Since physical region of s is $(v_b, 0)$, in order to avoid the 'spiral' curve, $(s_-, s_+) \cap (v_b, 0)$ needs to be an empty set. One can show that $s_+ < v_b$ for $w_1 > 8$. Consequently, the 'spiral' curve never happens.

Since we always have $D > 0$, the curve C in the (X_+, X_-) coordinates satisfies

$$X_\pm = X_{\pm,0} \left(\frac{r}{r_R}\right)^{\epsilon_\pm} \rightarrow \frac{X_-}{X_+} = \frac{X_{-,0}}{X_{+,0}} r^{-\sqrt{D}}, \tag{3.20}$$

where $X_{\pm,0}$ are integration constants. In other words, as r increases towards r_R, the curve changes gradually (not oscillating) to the limit $(X_{-,0}/X_{+,0}) r_R^{-\sqrt{D}}$.

This gives $X_+/X_{+,0} = (X_-/X_{-,0})^{\epsilon_+/\epsilon_-}$. For types I, II and V, where $\epsilon_\pm$ are real,

$$\epsilon_+ \epsilon_- = \frac{2w_2}{w_1} \left(1 + \frac{4w_2}{(1 + w_1)^2}\right) < 0.$$

This implies that every solution curve approaches along one of the $X_\pm$ axis and departs along the other axis without touching the point P_R. Note that for the type IV, the repelling point is located outside of the region we are interested in.
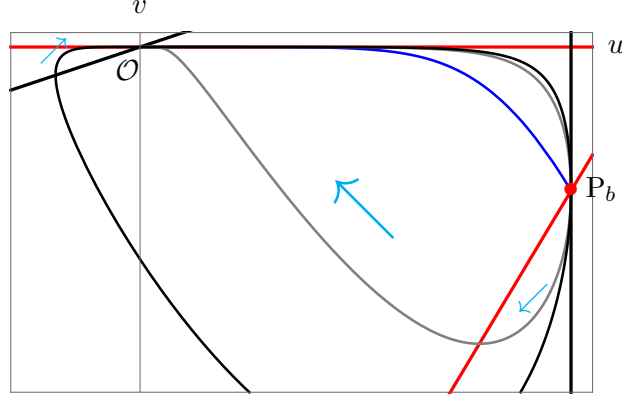
Figure 3. Numerical solutions for the Type I with $w_1 = -2$ and $w_2 = 1.5$.

4 Numerical solutions

In this section, we present and display numerical solutions of the Einstein's equation (2.10) on the (u, v) plane to show behaviors of solutions.

4.1 $w_1 < -1$ case

A regular wormhole made of an anisotropic matter with non-negative energy density exists only for the Type I, where $w_1 < -1$ and $w_2 > -(1 + w_1)/4$. A well-localized solution having finite total mass exists when $w_2 > -w_1/2$. Therefore, we restrict our interests only to this situation.

1. *Symmetric solution.* The blue curve in figure 3 corresponds to the linear behavior ii) at P_b in eq. (3.11). The curve represents half of the wormhole solution from the throat at P_b to an asymptotic region at $\mathcal{O}$. The other half of the wormhole can be added by duplicating the curve.

2. *Asymmetric solution.* Given a positive κ in eq. (3.10), an asymmetric solution curve is specified. The gray curve represents a solution corresponding to a regular wormhole. In this case, the geometry of the wormhole is not symmetric with respect to the throat. Any curve which begins at P_b and ends at $\mathcal{O}$ represents half of the spacetime including a throat and an asymptotic region. In the lower part of the gray curve, the value of u monotonically decreases and forms an asymptotically flat region at $\mathcal{O}$. While, for the case of the solution curve corresponding to the other half, v bounces back around P_R and starts to decrease. Then, it also forms the other asymptotically flat region at $\mathcal{O}$.

3. *Solution with one asymptotic region.* Two ends of the black curve go into the region $\mathcal{O}$ and $v \to \infty$, respectively. The wormhole throat is located at P_b. Following the upper part of the black curve, the radius increases to a finite value as $v \to \infty$. Therefore, a singularity of density exists.

Figure 4. Numerical solutions for the type IV with $w_1 = 2$ and $w_2 = -3$.

4.2 $w_1 > 0$ case

In this case, the energy density is negative definite. A regular wormhole solution exists only for the Type IV, where $w_2 < -(1 + w_1)/4$. A well localized solution having finite total mass exists when $0 < w_1 < -2w_2$. Therefore, we restrict our interests only to this situation.

1. *Symmetric solution.* The blue curve in figure 4 corresponds to the linear behavior ii) at P_b in eq. (3.11). The curve represents half of the wormhole solution from the throat at P_b to an asymptotic region at $\mathcal{O}$. The other half of the wormhole can be added by duplicating the curve.

2. *Asymmetric solution I.* The gray curve presents a solution curve corresponding a regular wormhole in which the mass function is positive definite in all the spacetime. In this case, the geometry is not symmetrical around the throat.

   In the upper part of the gray curve, the value of u monotonically increases and forms an asymptotically flat region at $\mathcal{O}$. While, for the case of the solution curve corresponding to the other half, u decreases at the beginning but bounces back and increases. Then, it also forms the other asymptotically flat region at $\mathcal{O}$.

3. *Asymmetric solution II.* Two ends of the black curve go into the point $\mathcal{O}$. In this case, one end of C approaches $\mathcal{O}$ starting from the negative value of u. Therefore, the mass function becomes negative in this region. Only the asymptotic behaviors around the point $\mathcal{O}$ are different from the first case.

5 Analytic solutions

Even though one cannot find a general solution of eq. (2.9) it is still possible to find a few new analytic solutions. In this section, we present two exact solutions for the cases $w_2 = -(1 + w_1)/2$ and $w_2 = -(1 + w_1)/4$.

5.1 Various solutions for the case $1 + w_1 + 2w_2 = 0$

First, we present an exact solution for the matter which marginally satisfies the strong energy condition $\rho + \sum_i p_i \geq 0$. That is, when $\rho + \sum_i p_i = (1 + w_1 + 2w_2)\rho = 0$, eq. (2.9) permits a solution. In this case, the slope $s = 1/2w_1 = -v_b$.
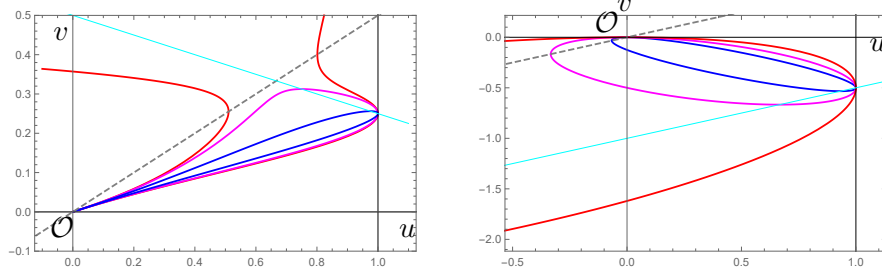
Figure 5. Various solution curves for $1 + w_1 + 2w_2 = 0$. (Left) The curves for $(w_1, w_2) = (-2, 1/2)$ for various $\lambda = 0.3, 0.64$, and 0.7 respectively for the blue, magenta and red curves; (Right) The curves for $(w_1, w_2) = (1, -1)$. Here $\lambda = 0.5, 1$ and 1.8, respectively for the blue, magenta and red curves. Every solution curves pass the point $(u, v) = (1, v_b)$ where a wormhole throat forms.

One can solve the TOV equation (2.9) in an explicit form:

$$\left| \frac{v}{v_b} - u \right| \left(\frac{v}{v_b} \right)^{-\frac{w_1}{1+w_1}} = \lambda \, (1 - u)^{1/2}, \tag{5.1}$$

where λ is a positive constant. One can confirm that this solution satisfies the autonomous equation (2.10) for $1 + w_1 + 2w_2 = 0$. The solutions $v(u)$ are characterized by the constant λ. We present various solutions $v(u)$ in figure 5.

Series expanding eq. (5.1) around the throat, gives κ:

$$\kappa = (v_b \lambda)^{-2}. \tag{5.2}$$

Given a solution $v(u)$, one can obtain $u(r), v(r)(\equiv v(u(r))$ as functions of r by using the eq. (3.4):

$$r = \exp \left(\int \frac{du}{2v(u) - u} \right). \tag{5.3}$$

One can readily check that, when $C = 0$, eq. (5.1) becomes a linear solution curve

$$v = v_b u. \tag{5.4}$$

In fact, one of the solution found in ref. [1] is a special case of the linear solution when $w_1 = -2$. This linear solution plays an important role in analyzing the solution space of eq. (2.10).

The radius and the density behaves as

$$r = b \left(\frac{v}{v_b} \right)^{-\frac{w_1}{1+w_1}}, \qquad \rho = \frac{v}{4\pi r^2} = \frac{v_b}{4\pi b^2} \left(\frac{b}{r} \right)^{3+\frac{1}{w_1}}. \tag{5.5}$$

At the point $\mathcal{O}(0, 0)$, the radius diverges to form a regular asymptotic region. At the point $r = b$, it forms a wormhole throat at $v = v_b$. The mass function becomes

$$m(r) = \frac{ru}{2} = \frac{b}{2} \left(\frac{r}{b} \right)^{-\frac{1}{w_1}}. $$

For $w_1 > 0$, the mass monotonically decreases from $b/2$ to zero as $r \to \infty$. Therefore, as $r \to \infty$, the total mass becomes divergent/zero when $w_1 \lessgtr 0$.
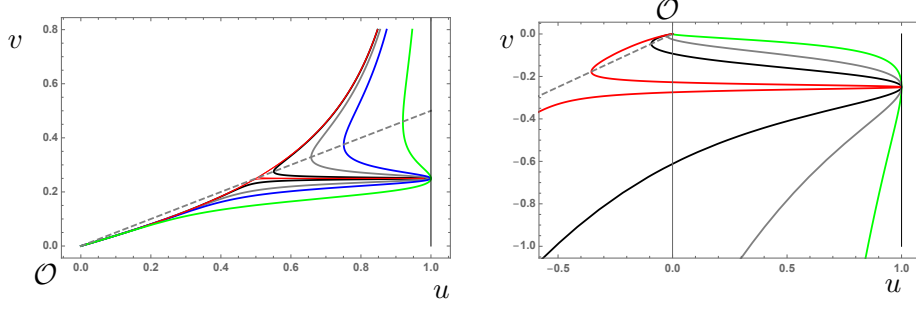
Figure 6. Various solution curves with $c_1 > 1$ for $(w_1, w_2) = (-2, 1/4)$ (Left) and $(2, -3/4)$ (Right). Here $c_1 = 1.001, 1.1, 1.5, 2$, and 4, respectively for red, black, gray, blue, and green curves. Every solution curves with $c_1 > 1$ pass the point $(u, v) = (1, v_b)$ where a wormhole throat forms.

The metric can be reconstructed to be

$$g_{tt}(r) = -f_0,$$
$$g_{rr}(r) = \frac{1}{1 - \left(\frac{b}{r}\right)^{(1+w_1)/w_1}}. \tag{5.6}$$

In other words the temporal component of the metric is independent of r. The radial component for the metric linearly diverges as $r \to b$, which is a signature of the wormhole throat.

5.2 Various solutions for the case $1 + w_1 + 4w_2 = 0$

A new analytic wormhole solution exists in this case. The strong energy condition will be violated for $w_1 < -1$ because $1 + w_1 + 2w_2 = -2w_2 < 0$. Since the slope $s = 0$, the denominator of eq. (2.10) has no u dependence and the equation is integrable exactly to give

$$u = 1 - \frac{\left(1 - \frac{v}{v_b}\right)^2}{1 + \frac{2w_1}{1-w_1}\left(\frac{v}{v_b}\right) - c_1 \frac{1+w_1}{1-w_1}\left(\frac{v}{v_b}\right)^{\frac{2w_1}{1+w_1}}}, \tag{5.7}$$

where c_1 is an integration constant.

The characteristic behaviors of the solution curves with $c_1 > 1$ are given in figure 6 in which $w_1 = 2$ and -2, respectively for the left and the right panels. We neglected the curves with $c_1 \leq 1$ because they do not contain a wormhole throat. For both the cases, one end of the solution curves finishes at $\mathcal{O}$, which corresponds to an asymptotic infinity at $r \to \infty$. The other end finishes at $v \to \infty$ or $(u, v) \to (-\infty, -\infty)$, respectively for $w_1 < -1$ or $w_1 > 0$, where a singularity forms.

Let us observe the behaviors of the solutions in detail. Around $v = v_b$, it becomes, for $c_1 \geq 1$,

$$u \approx 1 + \frac{4w_1^2}{(c_1 - 1)}\frac{1-w_1}{1+w_1}(v - v_b)^2, \quad c_1 > 1; \qquad u \approx -\frac{1}{w_1} - \frac{2(v/v_b - 1)}{3w_1}, \quad c_1 = 1.$$

Therefore, eq. (5.7) presents a relevant wormhole throat when $c_1 > 1$ because $u \leq 1$ in this case. On the other hand, when $c_1 = 1$, the curve does not pass the point $(u, v) = (1, v_b)$, the throat. Incidentally, the value of κ in eq. (3.10) is related with c_1 by

$$\kappa = \frac{4w_1^2}{1 - c_1}\frac{1-w_1}{1+w_1}.$$

– 15 –

Around $\mathcal{O}$, the asymptotic region, u behaves as

$$
u \approx \begin{cases}
\frac{2}{1-w_1} \frac{v}{v_b}, & |w_1| > 1, \\[3mm]
-c_1 \frac{1+w_1}{1-w_1} \left(\frac{v}{v_b} \right)^{\frac{2w_1}{1+w_1}}, & 0 < w_1 < 1, \\[3mm]
\frac{v}{v_b} \log \frac{c_1 v}{v_b}, & w_1 = 1.
\end{cases}
\tag{5.8}
$$

When $|w_1| > 1$, the linear behavior dominates. On the other hand, when $0 < w_1 < 1$, polynomial behavior dominates.

The radius can be obtained by using eqs. (2.10) and (3.4):

$$
r = b \left(\frac{v}{v_b} \right)^{-\frac{2w_1}{1+w_1}} \frac{1-w_1}{(1+w_1)(1-c_1)} \left(1 + \frac{2w_1}{1-w_1} \frac{v}{v_b} - c_1 \frac{1+w_1}{1-w_1} \left(\frac{v}{v_b} \right)^{\frac{2w_1}{1+w_1}} \right).
\tag{5.9}
$$

The radius takes its minimum value b at the throat $v = v_b$. As v decreases, the radius goes to infinity at $v = 0$. On the other hand, as $v \to \infty$ the radius increases to a local maximum value $bc_1/(c_1 - 1)$ or diverges with the form $r \propto v^{(1-w_1)/(1+w_1)}$, respectively for $|w_1| > 1$ or $0 < w_1 < 1$.

The mass function behaves as

$$
m = \frac{ur}{2} = \frac{b}{(1-c_1)(1+w_1)} \left(\frac{v}{v_b} \right)^{\frac{1-w_1}{1+w_1}} \left[1 - \frac{1-w_1}{2} \frac{v}{v_b} - c_1 \frac{(1+w_1)}{2} \left(\frac{v}{v_b} \right)^{-\frac{1-w_1}{1+w_1}} \right].
\tag{5.10}
$$

For $w_1 < -1$, the mass function has a divergent value for large r ($v \to 0$). This is a signature of the instability of the wormhole throat. The mass decreases to $m(v_b) = b/2$ and then bounces back to increase to a finite value $m(v \to \infty) = bc_1/2(c_1 - 1)$. For $w_1 > 1$, the mass diverges both at $v \to 0$ and as $v \to \infty$. On the other hand, for $0 < w_1 < 1$, it goes to a constant value $m(v = 0) = bc_1/2(c_1 - 1)$ at $v = 0$ but diverges as $v \to \infty$.

The $g_{tt}(\equiv -f)$ part of the metric function from eq. (2.8) becomes

$$
f(r) = f_0 \left(\frac{r}{r_0} \right)^{\frac{4(w_2 - w_1)}{1+w_1}} \left(\frac{\rho}{\rho_0} \right)^{-\frac{2w_1}{1+w_1}} = f_0 \left(\frac{r}{r_0} \right)^{\frac{4w_2}{1+w_1}} \left(\frac{v(r)}{v_0} \right)^{-\frac{2w_1}{1+w_1}}.
\tag{5.11}
$$

One may also check the two formula for $f(r)$ in eqs. (2.7) and (2.8) present the same result. The g_{rr} part of the metric function is

$$
g_{rr}(r) = \frac{1 + \frac{2w_1}{1-w_1} \left(\frac{v(r)}{v_b} \right) - c_1 \frac{1+w_1}{1-w_1} \left(\frac{v(r)}{v_b} \right)^{\frac{2w_1}{1+w_1}}}{\left(1 - \frac{v(r)}{v_b} \right)^2}.
\tag{5.12}
$$

Although the two exact solutions discussed in this section have deficits of their own, they provide good insights into the general solution space.

6 Limiting solution for $|s| \gg 1$

One can rewrite the TOV equation (2.10) as

$$
\frac{du}{dv} = \frac{-1}{1+w_1} \left(\frac{2v - u}{v} \right) \frac{1-u}{v - su - v_s}, \qquad v_s \equiv v_b - s = \frac{2w_2}{w_1(1+w_1)}.
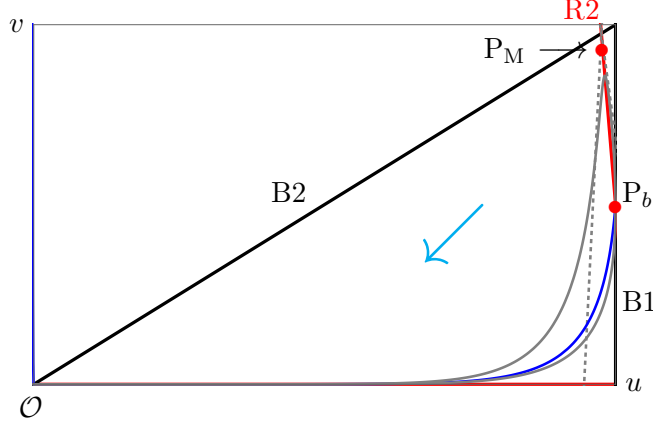\tag{6.1}
$$

Figure 7. Characteristic picture of limiting solution of Type I with $w_1 < -1$.

One can see that when the value of s is large, the value of v_s is also large. v_s can be rewritten as

$$v_s \equiv -as, \quad a \equiv \frac{4w_2}{1 + w_1 + 4w_2}. \quad (6.2)$$

Now, the TOV equation can be expanded as a series of s^{-1}

$$\frac{du}{dv} = \frac{-1}{1 + w_1} \frac{(2v - u)(1 - u)}{v[v - s(u - a)]}$$
$$= -\alpha \left(\frac{2v - u}{v} \cdot \frac{1 - u}{1 - u/a} \right) \left[1 + \frac{v}{a - u} s^{-1} + \cdots \right], \quad (6.3)$$

where $\alpha = 1/(1 + w_1)as = -w_1/2w_2$ was defined in eq. (3.6). The general behavior of the 0th order solution is the same as that of the solution around $\mathcal{O}$ given in eq. (3.6).

$$u = -\frac{2\alpha}{1 - \alpha} v + q \left(\frac{v}{v_b} \right)^\alpha, \quad (6.4)$$

where q is an integration constant. For a solution curve passing the point $\mathcal{O}$, we should take $\alpha > 0$ because $v^\alpha \to \infty$ when $\alpha < 0$. Note that when α is given, the trajectories are classified by q only.

In figure 7, characteristic picture of the limiting solution is given. The blue curve represents a regular wormhole solution which is symmetric with respect to the throat. As seen in the figure, the curve gradually decreases to $\mathcal{O}$ with r.

The gray curve in figure 7 represents an asymmetric wormhole solution which is regular over the whole spacetime when $w_1 < -1$. Considering the upper half of the curve starting from the point P_b, the value of v increases to a maximum value at P_M and then decreases to zero as one approaches the asymptotic region. Let the coordinates of P_M be (u_M, v_M). Then we have

$$\left. \frac{dv}{du} \right|_M = 0, \quad v_M = s(u_M - a), \quad a \equiv \frac{4w_2}{1 + w_1 + 4w_2}. \quad (6.5)$$

Let us introduce a new coordinates (x, y) around P_M as $u \equiv u_M + x, v \equiv v_M + y$. Then eq. (2.10) can be approximated for small $|x|, |y| \ll 1$ and $|y| \ll |sx|$ to be

$$\frac{dy}{dx} = -c_M \left[x + \left(\frac{1}{1 - u_M} + \frac{1}{2v_M - u_M} \right) x^2 + \cdots \right] \quad \Rightarrow \quad y = -\frac{1}{2} c_M x^2 + \mathcal{O}(x^3), \quad (6.6)$$

where

$$c_M = \left| \frac{(1+w_1)sv_M}{(1-u_M)(2v_M-u_M)} \right| = \left| \frac{a}{\alpha} \frac{v_M}{(1-u_M)(2v_M-u_M)} \right|. \tag{6.7}$$

The solution curve has approximately quadratic form around P_M, $y = -\frac{1}{2}c_M x^2$. As one moves farther from the maximum point, the curve takes higher order corrections.

When $|s|$ becomes large, the line R2 approaches the line B1, $a \to 1$ and $1-u_M \to 0$. For the asymmetric solution, the maximum point P_M goes near the repelling point P_R ($2v_M - u_M \to 0$). That is, $c_M \to \infty$. This means the solution curve becomes very steep and narrow as $|s| \to \infty$ as shown in figure 7. Hence, in the limit, the derivative of an asymmetric curve is discontinuous at P_M. As $u_M \to 1$, the curve mostly can be divided into the left part and the right part of P_M.

Solution curves around $\mathcal{O}$ are under the line B2 ($v < u/2$). Thus to meet P_M or P_b, derivative of the solution takes only positive value:

$$\frac{dv}{du} = \frac{1}{\frac{2\alpha}{\alpha-1} + \alpha q \left(\frac{v}{v_b}\right)^\alpha} = \frac{v}{\alpha(u-2v)} > 0, \tag{6.8}$$

for positive v. Therefore the type of solution (6.4) either can be extended to meet symmetric solutions (to P_b) or to meet the left part of the asymmetric solutions (to P_M) depending on the values of α and q.

7 Summary and discussions

We have classified static spherically symmetric wormholes consisting of an anisotropic matter throughout the entire spacetime and studied necessary conditions for the spacetime to be nonsingular. In the process, we found a few exact solutions in special configurations. We also presented wide variety of solutions by studying the properties they generally have. The behavior of wormhole geometry and physical quantities around important points such as the throat, the repelling point and the asymptotes have been studied. Numerical solutions have also been presented to give insights into the behaviors of general solutions.

We found that the throat geometry is insensitive to the angular pressure. The derivative of the mass function depends solely on the radial pressure as in eq. (2.13). The regular asymptotic geometry is determined by the ratio of the radial to the angular pressures.

An anisotropic matter with the limit $w_1 \equiv p_1/\rho \to -1$ resembles the stress-energy tensor of radial electric field which may be used to produce a charged wormhole in ref. [3]. This corresponds to the $|s| \to \infty$ limit which we analyzed in section 6. From the asymptotic form of the solution in eq. (6.4), the part of the solution near the maximum v_M in eq. (6.6) and the numerical solution, one can figure out how the solution behaves. However, we observed that there is no wormhole solution when $w_1 = -1$. One may wonder whether this is contradictory to the case that corresponds to a charged wormhole solution, for example, that in ref. [3]. There, the energy density and the pressure are given by

$$\rho = \rho^{(0)} + \rho^{(1)},$$
$$p_1 = p_1^{(0)} + p_1^{(1)}, \tag{7.1}$$

where $(\rho^{(0)}, p_1^{(0)})$ are those of non-charged wormhole solution and $(\rho^{(1)}, p_1^{(1)})$ are the charged dressing,

$$\rho^{(1)} = -p_1^{(1)} = \frac{Q^2}{8\pi r^4}, \tag{7.2}$$

where Q is the electric charge. As one can see in the above equation (7.1), $p_1 \neq -\rho$ or $w_1 \neq -1$ unless $\rho^{(0)} = p_1^{(0)} = 0$. As the authors pointed out in the paper, it corresponds to the $b(r) = 0$ case in the reference and the spacetime becomes the Reissner-Nordström solution.

One may also use our solutions to construct a new solution which use exotic matter minimally. In the vicinity of the throat, the truncated solution of the present work can be matched with a Schwarzschild solution outside with appropriate junction conditions [21]. Stability of wormholes has also been studied in part in the context of general relativity recently [29, 30]. Though the studies are not yet complete, it was shown that the Ellis type wormhole can be stable. As the stability of a black hole made physicist to consider black hole seriously, we expect the stability of a wormhole does the role.

Most studies of wormhole concentrate on finding a solution of the gravitational field equations. Recently the exact form of entropy function $S(r)$ for a self-gravitating anisotropic matter was obtained [31]. When a wormhole is made of an anisotropic matter of radius R and the throat radius is B, the entropy is given by a sum of $S_1(R) - S_1(B)$ in one side and $S_2(R) - S_2(B)$ in the other side of the wormhole. Though there have been a few studies, the wormhole thermodynamics should be addressed to have more clear picture.

In this work, we cannot avoid the use of exotic matter because we are based on the general relativity. The extension of the analysis to a modified theory of gravity is admirable.

Acknowledgments

References

[1] M.S. Morris and K.S. Thorne, *Wormholes in space-time and their use for interstellar travel: A tool for teaching general relativity*, *Am. J. Phys.* **56** (1988) 395 [INSPIRE].

[2] M.S. Morris, K.S. Thorne and U. Yurtsever, *Wormholes, Time Machines and the Weak Energy Condition*, *Phys. Rev. Lett.* **61** (1988) 1446 [INSPIRE].

[3] S.-W. Kim and H. Lee, *Exact solutions of a charged wormhole*, *Phys. Rev.* **D 63** (2001) 064014 [gr-qc/0102077] [INSPIRE].

[4] S.V. Sushkov, *Wormholes supported by a phantom energy*, *Phys. Rev.* **D 71** (2005) 043520 [gr-qc/0502084] [INSPIRE].

[5] F.S.N. Lobo, *Phantom energy traversable wormholes*, *Phys. Rev.* **D 71** (2005) 084011 [gr-qc/0502099] [INSPIRE].

[6] K.A. Bronnikov, K.A. Baleevskikh and M.V. Skvortsova, *Wormholes with fluid sources: A no-go theorem and new examples*, *Phys. Rev.* **D 96** (2017) 124039 [arXiv:1708.02324] [INSPIRE].

[7] A. Raychaudhuri, *Relativistic cosmology. 1.*, *Phys. Rev.* **98** (1955) 1123 [INSPIRE].

[8] V.P. Frolov and I.D. Novikov, *Physical Effects in Wormholes and Time Machine*, *Phys. Rev.* **D 42** (1990) 1057 [INSPIRE].

[9] C.W. Misner and J.A. Wheeler, *Classical physics as geometry: Gravitation, electromagnetism, unquantized charge and mass as properties of curved empty space*, *Annals Phys.* **2** (1957) 525 [INSPIRE].

[10] H.-C. Kim and Y. Lee, *Thermodynamic Equilibrium of a Wormhole Station*, arXiv:1902.02957 [INSPIRE].

[11] K.A. Bronnikov and V.G. Krechet, *Potentially observable cylindrical wormholes without exotic matter in general relativity*, *Phys. Rev.* **D 99** (2019) 084051 [arXiv:1807.03641] [INSPIRE].

[12] M.R. Mehdizadeh, M. Kord Zangeneh and F.S.N. Lobo, *Einstein-Gauss-Bonnet traversable wormholes satisfying the weak energy condition*, *Phys. Rev.* **D 91** (2015) 084004 [arXiv:1501.04773] [INSPIRE].

[13] M. Kord Zangeneh, F.S.N. Lobo and M.H. Dehghani, *Traversable wormholes satisfying the weak energy condition in third-order Lovelock gravity*, *Phys. Rev.* **D 92** (2015) 124049 [arXiv:1510.07089] [INSPIRE].

[14] S.H. Mazharimousavi and M. Halilsoy, *Wormhole solutions in $f(R)$ gravity satisfying energy conditions*, *Mod. Phys. Lett.* **A 31** (2016) 1650192 [INSPIRE].

[15] K.K. Nandi, A. Islam and J. Evans, *Brans wormholes*, *Phys. Rev.* **D 55** (1997) 2497 [arXiv:0906.0436] [INSPIRE].

[16] E.F. Eiroa, M.G. Richarte and C. Simeone, *Thin-shell wormholes in Brans-Dicke gravity*, *Phys. Lett.* **A 373** (2008) 1 [*Erratum ibid.* **373** (2009) 2399] [arXiv:0809.1623] [INSPIRE].

[17] H.B.G. Casimir, *On the Attraction Between Two Perfectly Conducting Plates*, *Indag. Math.* **10** (1948) 261 [INSPIRE].

[18] L.H. Ford and T.A. Roman, *Negative energy, wormholes and warp drive*, *Sci. Am.* **282N1** (2000) 30.

[19] J. Maldacena and L. Susskind, *Cool horizons for entangled black holes*, *Fortsch. Phys.* **61** (2013) 781 [arXiv:1306.0533] [INSPIRE].

[20] J. Maldacena, A. Milekhin and F. Popov, *Traversable wormholes in four dimensions*, arXiv:1807.04726 [INSPIRE].

[21] W. Israel, *Singular hypersurfaces and thin shells in general relativity*, *Nuovo Cim.* **B 44S10** (1966) 1 [*Erratum ibid.* **B 48** (1967) 463] [INSPIRE].

[22] M. Visser, *Lorentzian wormholes: From Einstein to Hawking*, AIP, Woodbury, U.S.A. (1995) [INSPIRE].

[23] H.-C. Kim, *Black hole in closed spacetime with an anisotropic fluid*, *Phys. Rev.* **D 96** (2017) 064053 [arXiv:1708.02373] [INSPIRE].

[24] I. Cho and H.-C. Kim, *Static-Fluid Black Holes*, *Phys. Rev.* **D 95** (2017) 084052 [arXiv:1610.04087] [INSPIRE].

[25] I. Cho and H.-C. Kim, *Simple black holes with anisotropic fluid*, *Chin. Phys.* **C 43** (2019) 025101 [arXiv:1703.01103] [INSPIRE].

[26] K.A. Bronnikov, *Scalar fields as sources for wormholes and regular black holes*, *Particles* **1** (2018) 56 [arXiv:1802.00098] [INSPIRE].

[27] S. Halder, S. Bhattacharya and S. Chakraborty, *Spherically symmetric wormhole solutions in a general anisotropic matter field*, *Phys. Lett.* **B 791** (2019) 270 [arXiv:1903.03343] [INSPIRE].

[28] R.D. Sorkin, R.M. Wald and Z.J. Zhang, *Entropy of selfgravitating radiation*, *Gen. Rel. Grav.* **13** (1981) 1127 [INSPIRE].

[29] K.A. Bronnikov, L.N. Lipatova, I.D. Novikov and A.A. Shatskiy, *Example of a stable wormhole in general relativity*, *Grav. Cosmol.* **19** (2013) 269 [arXiv:1312.6929] [INSPIRE].

[30] I. Novikov and A. Shatskiy, *On stability of a new model of wormhole*, arXiv:1201.4112 [INSPIRE].

[31] H.-C. Kim and Y. Lee, *Entropy of Self-Gravitating Anisotropic Matter*, *Eur. Phys. J.* **C 79** (2019) 679 [arXiv:1901.03148] [INSPIRE].